

The Vectorcardiogram and the Main Dromotropic Disturbances

Andrés R. Pérez-Riera^{1,*}, Raimundo Barbosa-Barros², Rodrigo Daminello-Raimundo¹, Luiz C. de Abreu^{1,3} and Kjell Nikus⁴

¹Laboratório de Delineamento de Estudos e Escrita Científica, Centro Universitário Saúde ABC, Santo André, São Paulo, Brazil; ²Coronary Center of the Hospital de Messejana Dr. Carlos Alberto Studart Gomes, Fortaleza, Ceará, Brazil; ³Graduate Entry Medical School, University of Limerick, Limerick, Ireland; ⁴Heart Center, Tampere University Hospital and Faculty of Medicine and Health Technology, Tampere University, Tampere Finland

ARTICLE HISTORY

Received: February 21, 2020
Revised: April 27, 2020
Accepted: April 27, 2020

DOI:
10.2174/1573403X16666200810105504

Abstract: Until the mid-1980s, it was believed that the vectorcardiogram (VCG) presented a greater specificity, sensitivity and accuracy in comparison to the 12-lead electrocardiogram (ECG), in the cardiology diagnosis. Currently, the VCG still is superior to the ECG in specific situations, such as in the evaluation of myocardial infarctions when associated with intraventricular conduction disturbances, in the identification and location of accessory pathways in ventricular preexcitation, in the differential diagnosis of patterns varying from normal of electrical axis deviation, in the evaluation of particular aspects of Brugada syndrome, Brugada phenocopies, concealed form of arrhythmogenic right ventricular cardiomyopathy and zonal or fascicular blocks of the right bundle branch on right ventricular free wall. VCG allows us to analyze the presence of left septal fascicular block more accurately than ECG and in the diagnosis of the interatrial blocks and severity of some chambers enlargements. The three-dimensional spatial orientation of both the atrial and the ventricular activity provides a far more complete observation tool than the linear ECG. We believe that the ECG/VCG binomial simultaneously obtained by the technique called electro-vectorcardiography (ECG/VCG) brought a significant gain for the differential diagnosis of several pathologies. Finally, in the field of education and research, VCG provided a better and more rational tridimensional insight into the electrical phenomena that occurs spatially, and represented an important impact on the progress of electrocardiography.

Keywords: Vectorcardiogram, electrocardiogram, dromotropic disturbances, left septal fascicular block, interatrial block, ventricular preexcitation.

1. INTRODUCTION

The vectorcardiogram (VCG) is the spatial representation of electromotive forces generated during cardiac activity analyzed in three spatial planes. Consequently, the method provides three-dimensional information of the electric activity of the atria and the ventricles. VCG has advantages over the electrocardiogram (ECG); the spatial orientation and the magnitude of the vectors give a better idea of the magnitude and direction of electrical forces at any moment. Additionally, the VCG is still superior to the ECG in specific situations, such as to differentiate left anterior fascicular block (LAFB) from inferior myocardial infarction (MI) with left axis deviation [1], which is important for more accurate diagnosis of chamber enlargement and fascicular blocks associated with MI. LAFB is always accompanied by counterclockwise (CCW) inscription of the QRS loop whereas inferior MI invariably has clockwise (CW) inscription of the loop. Studies have shown the VCG to be more sensitive to the diagnosis and localization of infarction than the ECG [2]. When properly utilized, VCG should remain a

valuable diagnostic as well as a teaching tool [3]. VCG has greater specificity and sensitivity related to ECG for the diagnosis of chamber enlargement, fascicular blocks, and ventricular pre-excitation in association with MI. It is useful in diagnosing the coexistence of fascicular blocks and inferior MI. ECG criteria for the diagnosis of inferior wall MI are highly specific, but insensitive compared with VCG criteria [4]. In the fields of education and research, VCG provides a better insight into the electrical phenomena that occur spatially, and has an important impact on the progress of electrocardiographic science. We hope that the use of this resource will not get lost over time, since VCG still represents a source to enrich science by enabling a better morphological interpretation of the electrical phenomena.

In the present review, we will analyze the VCG characteristics of atrial and ventricular conduction disorders such as complete interatrial block (IAB), left and right bundle branch block (RBBB), left fascicular blocks and ventricular preexcitation.

2. COMPLETE, ADVANCED OR THIRD-DEGREE IAB

In these cases, the stimulus is blocked in the Bachmann bundle (BB) region, and the left atrium (LA) is retrogradely

* Address correspondence to this author at the School of Medicine, Centro Universit, Av. Lauro Gomes, 2000 - Vila Sacadura Cabral, Santo André, São Paulo, Brazil; E-mail: riera@uol.com.br

activated with a P wave duration ≥ 120 ms and plus-minus (+/-) P wave in the inferior leads II, III and aVF. There is an open angle $\geq 90^\circ$ between the vector of the first and second part of the P wave in the inferior leads. Orthogonal Y lead plus-minus with a negative mode >40 ms appear with notches and slurs in the last part of the P loop. IAB is often associated with left atrial enlargement (LAE) (up to 90% of cases) and dysfunction, decreased left ventricular (LV) filling [5], propensity for LA appendage thrombosis, increased atrial natriuretic peptide levels, and is a predictor of paroxysmal supraventricular tachyarrhythmias such as atrial fibrillation (AF), atrial flutter as well as an exacerbation of LV failure [6]. First degree IAB is much more frequent than complete IAB. In first degree IAB, the P-wave duration is 120 milliseconds or more, and the P waves are usually bimodal, especially in leads I, II and III. In addition, the final part of the P wave in lead V1 is negative although there is no left atrial enlargement (LAE), because the P loop is less posteriorly directed than in LAE, where the negative part of the P wave is deeper. The ECG pattern of complete IAB is an extremely strong marker of supraventricular tachyarrhythmia much more so than the presence of first degree or partial IAB. Bayés de Luna *et al.* [7] studied 16 patients with ECG evidence of complete IAB, eight patients with valvular heart disease, four with dilated cardiomyopathy and four with other forms of heart disease. Patients with valvular heart disease and cardiomyopathy were compared with a control group of 22 patients with similar clinical and echocardiographic characteristics, but without this type of IAB. Patients with complete IAB (ECG signs of retrograde activation of the LA) had a much higher incidence of paroxysmal supraventricular tachyarrhythmias during follow-up than did the control group. Eleven of 16 patients with complete IAB had atrial flutter (atypical in seven cases, typical in two cases, and with two or more morphologies in two cases). Six patients from the control group had sustained atrial tachyarrhythmias (five AF and one typical atrial flutter). Evidently, the atrial tachyarrhythmias were due more to advanced IAB and retrograde activation of LA and frequent premature atrial contractions (PACs) than to LAE, because the control group with a LA of the same size, but without complete IAB and retrograde activation of LA and with less incidence of PACs, had a much lower incidence of paroxysmal tachycardia.

Bayés de Luna *et al.* [8] demonstrated the value of preventive antiarrhythmic treatment in patients with complete IAB. In this population, LAE is present in 90% of cases.

From 81,000 ECGs, Bayes de Luna *et al.* [9] collected 83 cases that fulfilled the criteria of Interatrial Conduction Disturbances with Left Atrial Retrograde Activation (I-ACD-LARA) (P +/- in II, III and VF with P width ≥ 120 ms); this is equivalent to complete IAB. The authors presented a detailed study of 35 cases with surface ECG/VCG and 29 cases with orthogonal ECG leads. Two control groups were included: one with (30 cases) and one without known heart disease (25 cases). The prevalence of IACD-LARA was nearly 1% in the whole study population and 2% among patients with valvular heart disease. Arrhythmias, such as

AF and atrial flutter, were observed in $>90\%$ of the patients with complete IAB.

Diagnosis criteria of complete IAB and retrograde activation of the LA [7, 10-12]:

- Biphasic, bifid, or notched “plus-minus” P waves in the inferior leads II, III and aVF of the ECG and Y orthogonal lead of VCG.
- ECG: P-wave duration ≥ 120 ms.
- VCG: angle between the first portion (RA) and end portion (LA) $>90^\circ$.
- VCG: orthogonal Y lead plus-minus with the final negative portion ≥ 40 ms.
- ≥ 40 ms final portion of the P loop is located below the X and Z leads orthogonal X and Z leads.
- VCG: delayed final portion of the P loop, notches and slurring in the last part of the P loop.
- High esophageal lead recording: positive P wave polarity and P-wave delay.
- Low esophageal lead recording: plus-minus P wave polarity and P-wave delay.
- Intracavitary ECG recording: P wave craniocaudal activation inside the RA.
- Intracavitary ECG recording: P wave caudal-cranial activation inside LA.

Complete IAB should be considered as the ECG/VCG manifestation of the Bayés' Syndrome [13] (Fig. 1).

3. VCG FEATURES OF COMPLETE RIGHT BUNDLE BRANCH BLOCK

The VCG of complete RBBB (CRBBB) takes into account only the QRS loop in the horizontal plane (HP). There are three recognized VCG patterns: Grishman or Kennedy type I, Cabrera or Kennedy type II, and Kennedy type III or C (Fig. 2).

In the three patterns, the terminal vector of 60 to 120ms or more have “glove finger” shape (finger-like terminal appendix) located in the right anterior quadrant in the HP. The Cabrera or Kennedy type II pattern is frequently associated with moderate right ventricular hypertrophy (RVH), and Kennedy type III or C with severe RVH [17].

4. POSSIBLE ETIOLOGIES OF COMPLETE RIGHT BUNDLE BRANCH BLOCK

Normal variant: The incidence is 1.8 per 1,000. Below age 30 the incidence is 1.3 per 1,000 and between ages 30 and 44 it ranged from 2.0 to 2.9 per 1,000 (Hiss 1962), RBBB and incomplete RBBB (IRBBB) were two to three times more common among men than women. RBBB was associated with increased cardiovascular risk and all-cause mortality, whereas IRBBB was not. Contrary to common perception, RBBB in asymptomatic individuals should alert clinicians to consider the increased risk for cardiovascular events [18].

Congenital Heart Diseases: Associated diseases are: atrial septal defects (in more than 90% of cases), both the

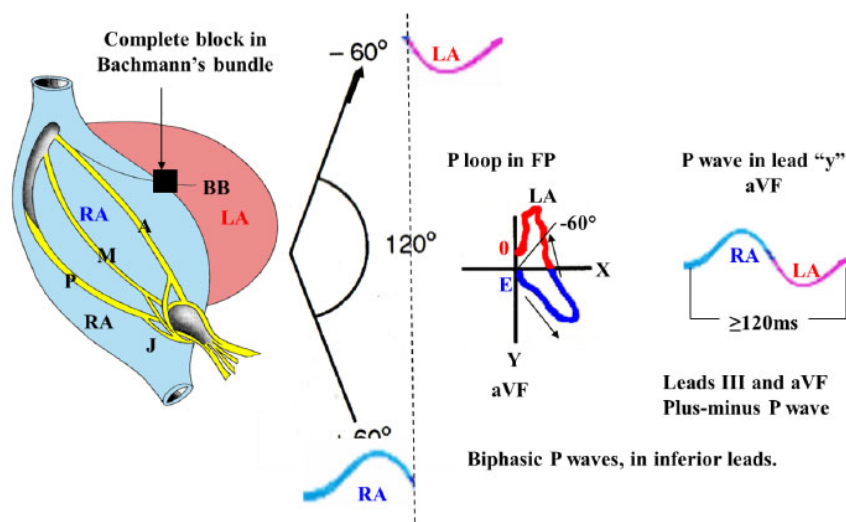


Fig. (1). Anatomic and ECG/VCG aspects of complete interatrial block. The electrical impulse is blocked/delayed in the BB region, but retrograde left atrial activation usually occurs [14]. Note the existence of an open angle between the vector of the first (RA) and the last (LA) portion of the P wave. Retrograde activation of the LA has been demonstrated in electrophysiological studies [15]. Consequently, P loop/wave in the orthogonal lead “Y”, aVF and III is biphasic plus-minus. LA activation occurs by an alternate route rather than proceeding from right to left *via* the BB [16]. A = anterior internodal pathway, M = middle internodal pathway, P = posterior internodal pathway, FP = frontal plane. (A higher resolution / colour version of this figure is available in the electronic copy of the article).

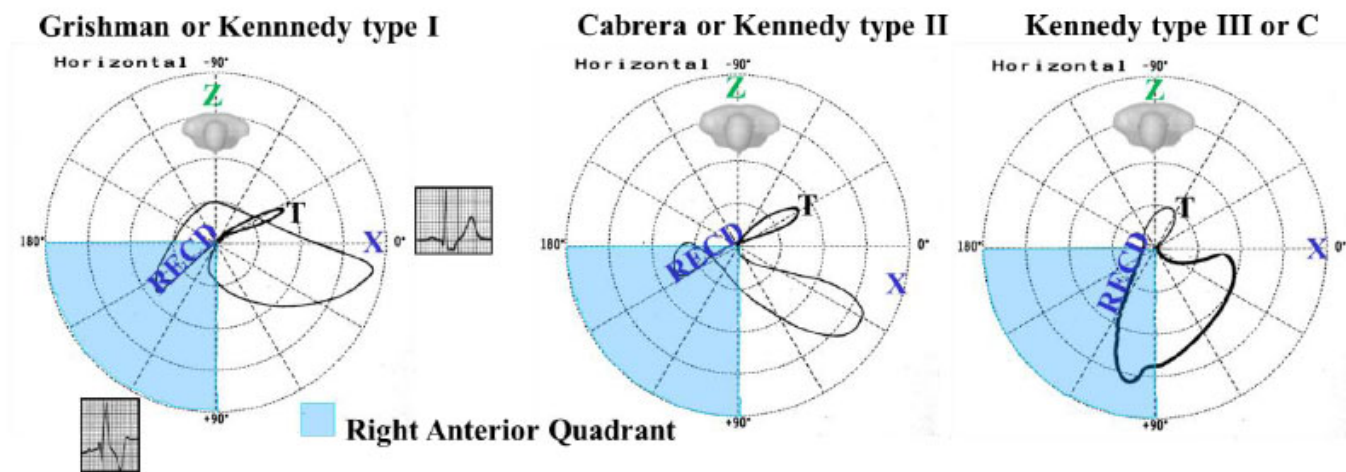


Fig. (2). VCG patterns of complete right bundle branch block. In the three patterns, the terminal vector of 60 to 120ms or more have “glove finger” shape (finger-like terminal appendix) located in the right anterior quadrant in the horizontal plane. The Cabrera or Kennedy type II pattern is frequently associated with moderate right ventricular hypertrophy (RVH), and Kennedy type III or C with severe RVH [17]. RECD: right end conduction delay. (A higher resolution / colour version of this figure is available in the electronic copy of the article).

ostium secundum and the ostium primum type [19]; partial or total anomalous pulmonary vein drainage to the right atrium; Ebstein’s anomaly [20]; Uhl’s anomaly [21]; ventricular septal defects (VSDs) in the presence of biventricular hypertrophy; pulmonary stenosis, especially in the moderate form and particularly in pulmonary stenosis of tetralogy of Fallot (ToF) or large VSD [22]; ToF (pre- and post-surgery) [23]; aortic stenosis: congenital, bivalvular, degenerative; after al-

cohol injection into the first septal perforator branch of the left anterior descending (LAD) coronary artery in hypertrophic obstructive cardiomyopathy [24].

Genetic-familial causes: Brugada syndrome: atypical CRBBB, frequently with the absence of wide S wave in the left precordial leads and ST segment elevation from V1 to V3 (SCN5A gene). Additionally, Brugada syndrome can be masked by CRBBB [25].

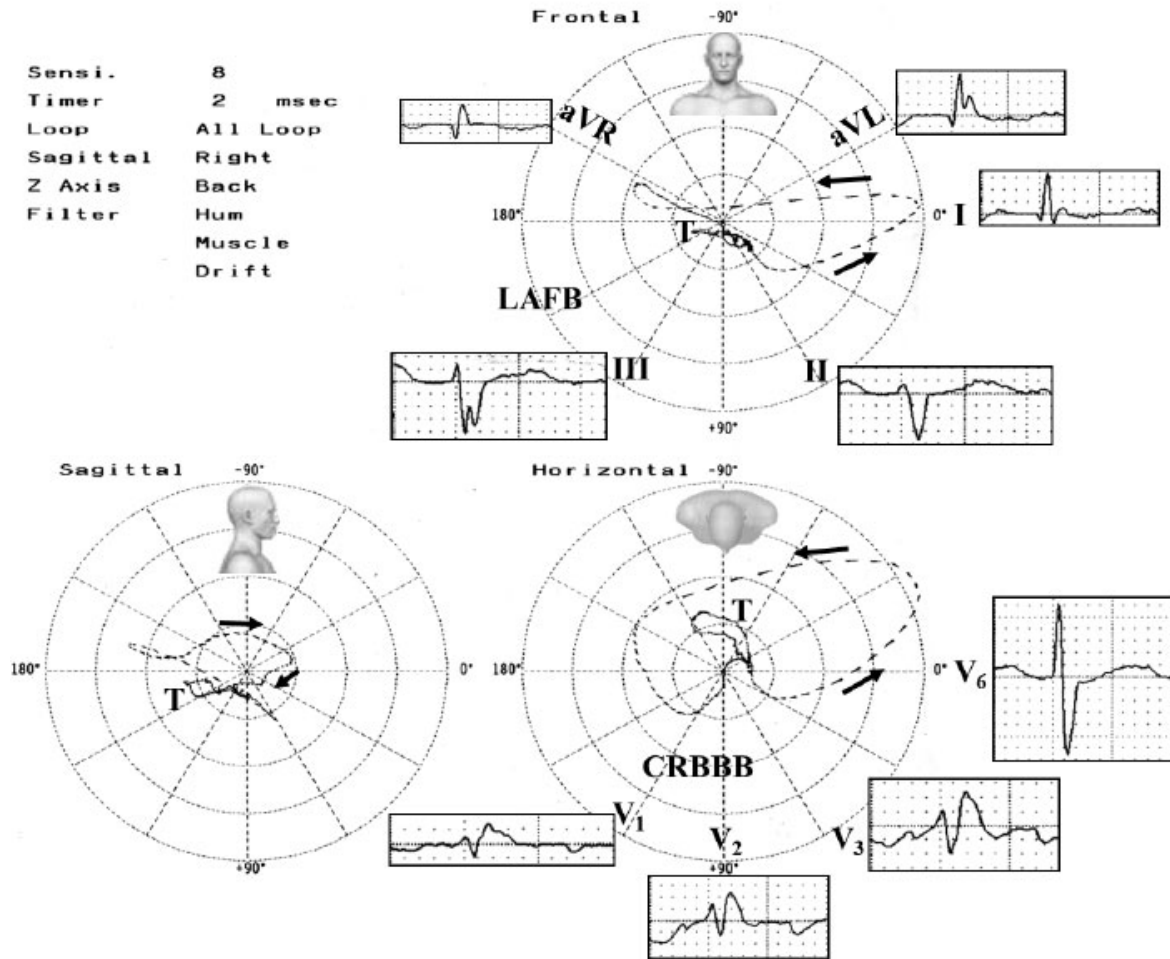


Fig. (3). Clinical diagnosis: Chronic chagasic myocarditis. **VCG diagnosis:** Extreme left axis deviation as a consequence of left anterior fascicular block (LAFB) associated with complete right bundle branch block (CRBBB) Grishman type observed in the horizontal plane. LAFB+RBBB is a typical pattern of chronic chagasic myocarditis.

VCG: Extreme left axis deviation as a consequence of LAFB associated with CRBBB Grishman type observed in the HP. LAFB+RBBB is a typical pattern of chronic chagasic myocarditis.

LAFB+RBBB constitutes the most frequent type of bifascicular block. In developed countries, the prevalence in the general population is ~1.4%. (A higher resolution / colour version of this figure is available in the electronic copy of the article).

5. RBBB ASSOCIATED WITH LEFT ANTERIOR FASCICULAR BLOCK

The initial portion of the loop behaves as a left anterior fascicular block (LAFB) and the final part as a CRBBB. The duration of the QRS loop ≥ 120 ms.

Frontal plane (FP): Very similar to isolated LAFB loop: initial vectors from 10 to 20ms heading downward and to the right (type I) or downward and to the left (type II); QRS loop of CCW rotation; QRS axis in the frontal plane (S \hat{A} QRS) with extreme deviation to the left beyond -30° ; an efferent branch of the QRS loop heading to the left and finally to the left and upward; an afferent branch that begins above and slightly to the left, to finally end in a final appendage of slow recording and located to the right and above.

HP: Typical QRS loop of a CRBBB [26]; vectors from initial 10 to 20 ms heading to the front and the right or left [27]; an efferent branch of QRS loop from right to left and with variable degrees of anteriorization; the main body of QRS loop with CCW (type I), eight or CW rotation (type II). The type of rotation seems to lack clinical significance; however, type II appears in a greater number of patients in chronic heart failure; the afferent branch of the QRS loop in front of the X line from left to right; the efferent branch of the QRS loop behind or in front of the X line; end delay located in the right anterior quadrant [28, 29]; ventricular repolarization with the T loop opposite to the final portion of the QRS loop to the left, behind and below [30] (Fig. 3).

LAFB+RBBB is the hallmark of chronic chagasic myocarditis, which constitutes the most frequent association in

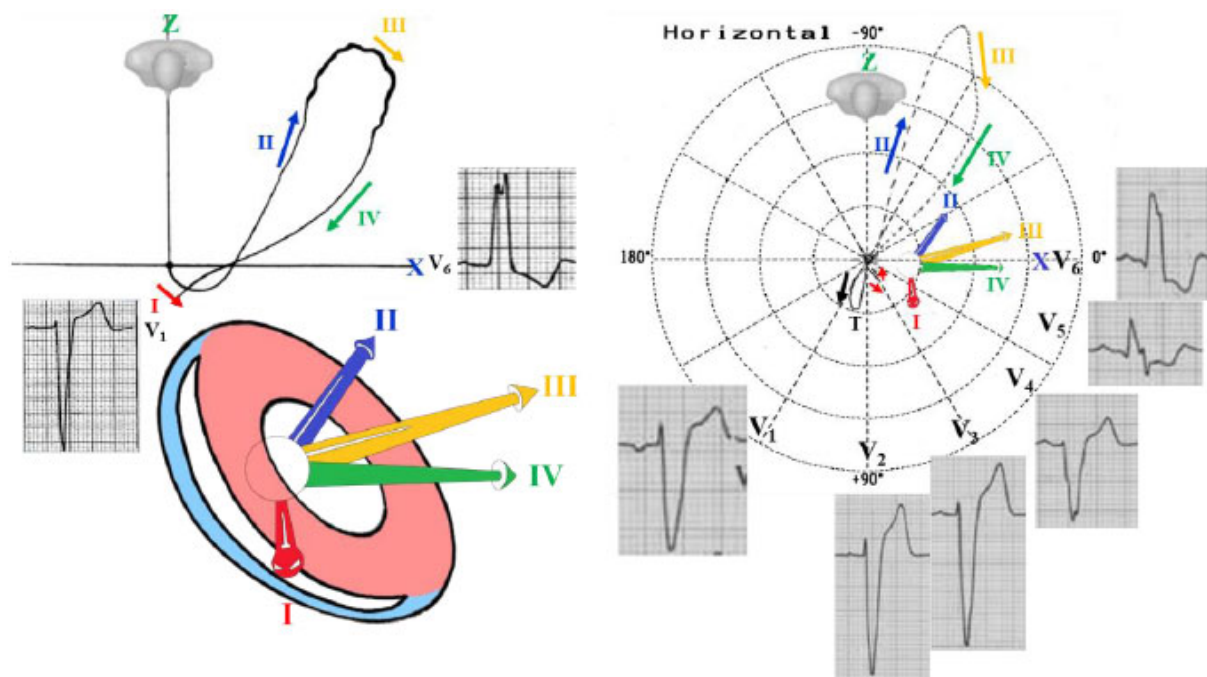


Fig. (4). ECG/VCG aspects of left bundle branch block. **VCG criteria in the HP:** Narrow, long QRS loop, and with morphology usually in “eight”; the QRS loop duration is ≥ 120 ms; the QRS loop shape is elongated and narrow; the main body of the QRS loop is inscribed posteriorly and to the left within the range of -90 to -40° ; maximal vector of QRS located in the left posterior quadrant (between -40° to -80°) and of increased magnitude (>2 mV); the main portions of the QRS loop of CW rotation. CCW rotation may indicate parietal CLBBB or association with lateral infarction or severe left ventricular hypertrophy (LVH); the efferent limb (II) located to the right related to the afferent limb (III and IV); conduction delay noted in the mid and terminal portion; the main body of QRS loop is inscribed CW; the magnitude of the max QRS vector is increased above normal exceeding 2mV; the ST segment and T wave vector are directed rightward and anteriorly; the T loop of CCW recording. The CW rotation of T wave in this plane suggests CLBBB complicated with infarction or LVH [33]. (A higher resolution / colour version of this figure is available in the electronic copy of the article).

Latin America, where it exists from the Argentinean Patagonia up to the frontier with the USA. In CRBBB of chronic chagasic myocarditis, a strong association (70% prevalence) with LAFB stands out. In patients younger than 40 years, from the endemic area, with CRBBB + LAFB, there is a high suspicion of chronic chagasic myocarditis, and even more with the additional presence of polymorphic ventricular extrasystoles and primary alterations of ventricular repolarization. The most frequent ECG pattern is typical (His bundle) CRBBB and LAFB. A longitudinal study of 5,710 infected patients showed that the presence of CRBBB associated with primary alterations of repolarization and electrically inactive areas indicates a high risk of death. Autopsy studies conducted by Andrade revealed that most of the patients with chronic chagasic heart disease present a significant involvement of the conduction system at the level of the nodal-His bundle (N-H) region of the AV node, the right penetrating and branching portion of the His bundle, proximal portion of the right bundle branch (RBB) and the left anterior fascicle (LAF) of the left branch. CRBBB of chronic chagasic heart disease is of the proximal type [31]. The most common ECG changes are the following: CRBBB (35%) and LAFB (35%). RBBB with LAFB is strongly related to Chagas disease in older patients [32].

6. OTHER ETIOLOGIES OF LAFB + RBBB

The prevalence of LAFB + RBBB in coronary heart disease (CHD), which represents the main cause in the developed countries, was $\sim 1\%$ in the hospital population. Post-myocardial infarction (MI), the prevalence is $\sim 6\%$, almost always caused by obstruction of the LAD, since the RBB and the LAF are irrigated by the perforator branches of this artery. Other etiologies are: hypertensive heart disease (in 20 to 25%); sclerodegenerative disease of the His system, genetic Lenègre disease with or without high blood pressure; Lev disease or sclerosis of the left side of the cardiac skeleton; and chest trauma. Closed trauma of the chest is frequently accompanied by CRBBB. In this case, the CRBBB frequently disappears after some hours. LAFB and RBBB may also appear in a familial form with syncope or sudden death, or it may be congenital and isolated. It may be associated with non-chagasic myocarditis; sarcoidosis; granulomatosis; aortic valve disease; hyperkalemia or hyperpotassemia; progressive external ophthalmoplegia. Post-surgery this bifascicular block may be seen:

- After corrective surgery of ToF (7 to 25% of the cases). It is of truncal type and indicates that the LAF has been injured during patch saturation to increase

the size of the right ventricular outflow tract. The patients that remain with bifascicular block after corrective surgery do not have a higher late mortality risk.

- In 4% of patients after corrective surgery of VSD.
- After tricuspid valve surgery.
- After bypass surgery with internal thoracic arterial and/or saphenous vein grafts (4%). CRBBB in isolation was observed in 6% and LAFB in 6%.

7. VCG IN COMPLETE LEFT BUNDLE BRANCH BLOCK (CLBBB)

The VCG diagnosis is made by using the HP (Fig. 4).

Possible etiologies of CLBBB: Systemic hypertension (SH) [34]; CHD [35]; association of SH and CHD; cardiomyopathies: in idiopathic dilated cardiomyopathy CLBBB is observed in $\approx 25\%$ of cases [36, 37]; diffuse myocardial disease; myocarditis; aortic valve disease [38]; mitral valve disease [39]; sclerosis of the left side of the cardiac skeleton: Lev disease [40]; familial progressive cardiac conduction defect (PCCD), “idiopathic” sclerosis of the His conduction system or Lenègre disease. Several genes, such as SCN5A [41], SCN1B and TRPM4, may be involved and result in familial PCCD [42]. It is usually inherited in an autosomal dominant matter, but also autosomal recessive inheritance and sporadic cases have been reported. Rare LBBB etiologies are: cardiomyopathies associated with collagenous disease [43]; congenital heart diseases (late phase of aortic stenosis); blood or crystalloid cardioplegia; use of taxol, cytotoxic antineoplastic drugs [44]; primary amyloidosis [45]; sarcoidosis [46]; hyperpotassemia [47]; postoperatively in hypertrophic obstructive cardiomyopathy [24]; after coronary angiography [48]; without apparent cause (idiopathic, cryptogenetic, primary or essential).

8. VCG CHARACTERISTICS OF FASCICULAR BLOCKS: LEFT ANTERIOR, POSTERIOR, AND SEPTAL FASCICULAR BLOCK

LAFB and left posterior block are mainly diagnosed by alterations in the FP. In contrast, LSFb affects only the HP (Fig. 5).

9. VCG IN VENTRICULAR PREEXCITATION

The VCG findings in ventricular pre-excitation are characterized by QRS loop conduction delay during the initial period of depolarization or slowing of the inscription in the initial part of the QRS loop. In other words, there is an initial slurring of the QRS complex due to the spread of activation from atria to ventricles *via* an accessory pathway (AP). This portion is called the delta (δ) vector. When the AP has a posterior location (formerly named Wolff-Parkinson-White [WPW] type A), the vector is directed anteriorly between 0° and $+90^\circ$, but occasionally to the right of $+90^\circ$. The maximal QRS vector is directed to the left and anteriorly in the majority of cases. In about 25% of cases, the maximal QRS vector is directed posteriorly in the HP. This subgroup may have LVH in addition to pre-excitation.

In the HP, the initial deflection is directed anteriorly and usually to the left, although occasionally to the right. The ef-

ferent limb proceeds to the left and relatively far anteriorly and then the loop turns in a CCW direction, the afferent limb passing behind the efferent limb to return on the right and anteriorly. Occasionally the entire HP QRS loop is inscribed in the CW direction and lies anteriorly and to the left. The maximal mean instantaneous vector of the HP QRS loop ranges in orientation between $+20^\circ$ and $+95^\circ$ in the majority of cases. In approximately 25% of patients, the maximal QRS vector is posteriorly located between -65° and 0° .

The frontal QRS loop tends to vary widely in configuration, although figure-eight loops are relatively common. Occasionally the frontal QRS loop has an almost linear configuration. The maximal mean instantaneous vector of the frontal QRS loop is usually located between -30° and $+100^\circ$. The initial deflection or δ vector may be superiorly or inferiorly directed. A superiorly oriented force will simulate an inferior MI if the initial conduction delay is not appreciated (Fig. 6).

The records are quite characteristic of the ventricular pre-excitation pattern with posterior AP (previously named type A ventricular pre-excitation). The δ vector is directed anteriorly and the QRS loop is located almost entirely in the anterior left quadrant. The T loop is oriented to the left and downward.

On the other hand, when the AP is located anteriorly (previously named type B WPW), the initial δ deflection in the HP is usually directed posteriorly. The characteristic conduction delay and irregular inscription are evident in the early part of the QRS loop and each projection. Generally, the efferent limb of the QRS loop is directed to the left and posteriorly. The loop then turns in the CCW direction more posteriorly and to the left, and it remains in this quadrant until the inscription is completed. The maximal instantaneous vector of the HP QRS loop lies between 0° and -90° .

In the FP, the δ vector and the remaining QRS loop are oriented to the left, either superiorly or inferiorly. The QRS loop may be inscribed in CW, CCW or in figure-eight configuration. The maximal mean instantaneous vector of the frontal loop is generally situated between -45° and -30° .

Ebstein’s anomaly is associated with the WPW syndrome (type B according to the old nomenclature) in 5 to 25% of cases, and it may be associated with left axis deviation. Ebstein’s anomaly is the congenital heart disease most frequently associated with WPW.

Patients with left-sided APs rarely show organic heart disease, while in 45% of the right-sided APs, there is an association with organic heart disease [51]. The locations of the AP in Ebstein’s anomaly are: right anterior (the most frequent one), right lateral, right posterior and right posteroseptal.

There are rare cases of Ebstein’s anomaly with pre-excitation of the Mahaim type: normal PR interval with δ wave that resembles CLBBB. Ebstein’s anomaly with CLBBB may correspond to the Mahaim type of pre-excitation. Mahaim pre-excitation is due to fibers that involve the His-nodal system, either from the AV node, or from the His bundle or its branches, expressed as two variants: ventricular nodal (connections) and fasciculoventricular (tracts).

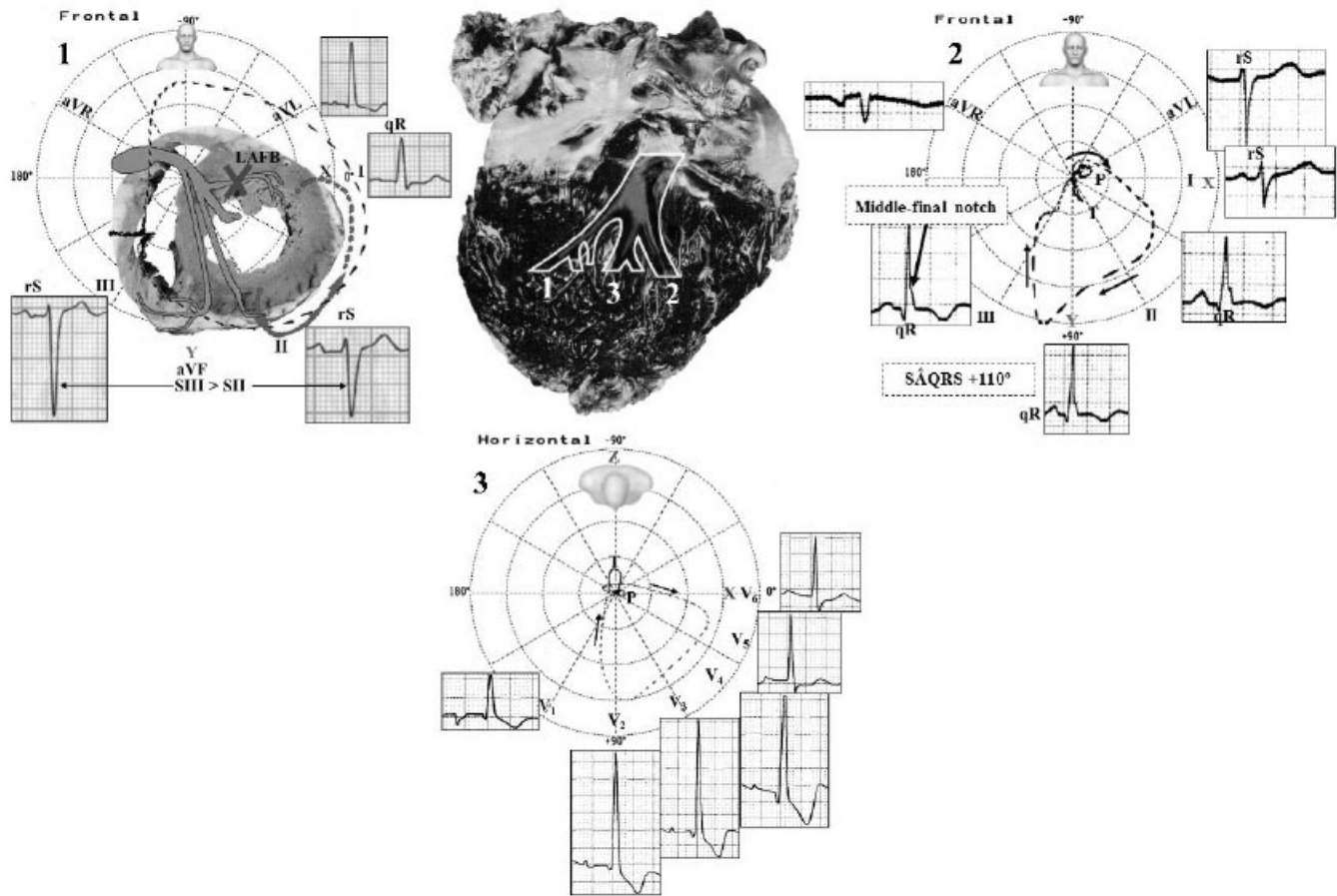


Fig. (5). LAFB (1): VCG in the FP: QRS loop ≤ 100 ms. When intermittent, the increase does not exceed 20 ms; constant CCW rotation of QRS loop when not associated with other diseases; in the presence of LVH or anterior MI, the rotation of the initial 20 ms may change; vector of initial 10 to 20 ms heading inferiorly; maximal vector of QRS heading superiorly around -20° ; QRS loop located in the left superior quadrant; ST/T loop always normal in non-complicated LAFB;

LPFB (2): VCG in the FP: Vector of initial 10 to 20 ms heading superiorly and to the left (near -45°) with possible delay (initial 10 to 25 ms). When associated with inferior MI, superior initial forces of ≥ 25 ms (more than 12.5 dashes above the orthogonal X lead. 1 dash = 2 ms) [49]; broad QRS loop, with CW rotation. According to Cooksey, Dunn and Massie, it may occasionally be in “eight” with a CCW terminal portion (10%); maximal vector near $+110^\circ$ ($+80^\circ$ to $+140^\circ$); almost all the loop is located below the X line (0 to $\pm 180^\circ$) in inferior quadrants; 20% of the loop located in the right inferior quadrant. If there is an association with CRBBB, 40% or more; afferent limb heading below and slightly to the left, and the efferent one to the right; middle-terminal portion of the QRS loop (vector of 60 ms to 100 ms) with delay. It may possibly reach the right superior quadrant; QRS loop duration up to 110 ms if in isolation. In association with CRBBB, >120 ms; normal ST-T vectors in isolated LPFB: T loop with CW rotation, heading inferiorly and to the left. If in association with CRBBB: alteration secondary to ventricular repolarization;

LPFB in the HP: QRS loop very similar to RVH of type C; QRS loop of CCW rotation. The rotation can be in “eight”; vector of initial 10 to 20 ms heading to the front and the right or left; greater area of QRS loop located in the left posterior quadrant; maximal vector of QRS around -60° to -110° ; final portions with delay (60 ms to 100 ms) and located in the right posterior quadrant; 20% or more of the area of the QRS loop located in the right posterior quadrant; and T loop to the front and the left ($+60^\circ$) and CW rotation;

LSF-B (3): The ECG/VCG modifications are observed only in the HP/precordial leads [50]. QRS loop in the HP with an area predominantly located in the left anterior quadrant ($\geq 2/3$ of the loop is facing the orthogonal X lead: 0° to $\pm 180^\circ$); absence of normal convexity to the right of the initial 20 ms of the QRS loop; discrete dextro or rightward-orientation with a moderate delay of the vector from 20 to 30 ms; anterior location of the 40 to 50 ms vector; posterior location with a reduced magnitude of the vector from 60 to 70 ms; maximal vector of the QRS loop located to the right of $+30^\circ$; intermittent anterior displacement of the QRS loop; The QRS loop rotation may be CCW (incomplete LSF-B) or CW: in advanced or complete LSF-B or in association with CRBBB, the T loop has a tendency to posterior orientation (useful for the differential diagnosis with lateral MI). (A higher resolution / colour version of this figure is available in the electronic copy of the article).

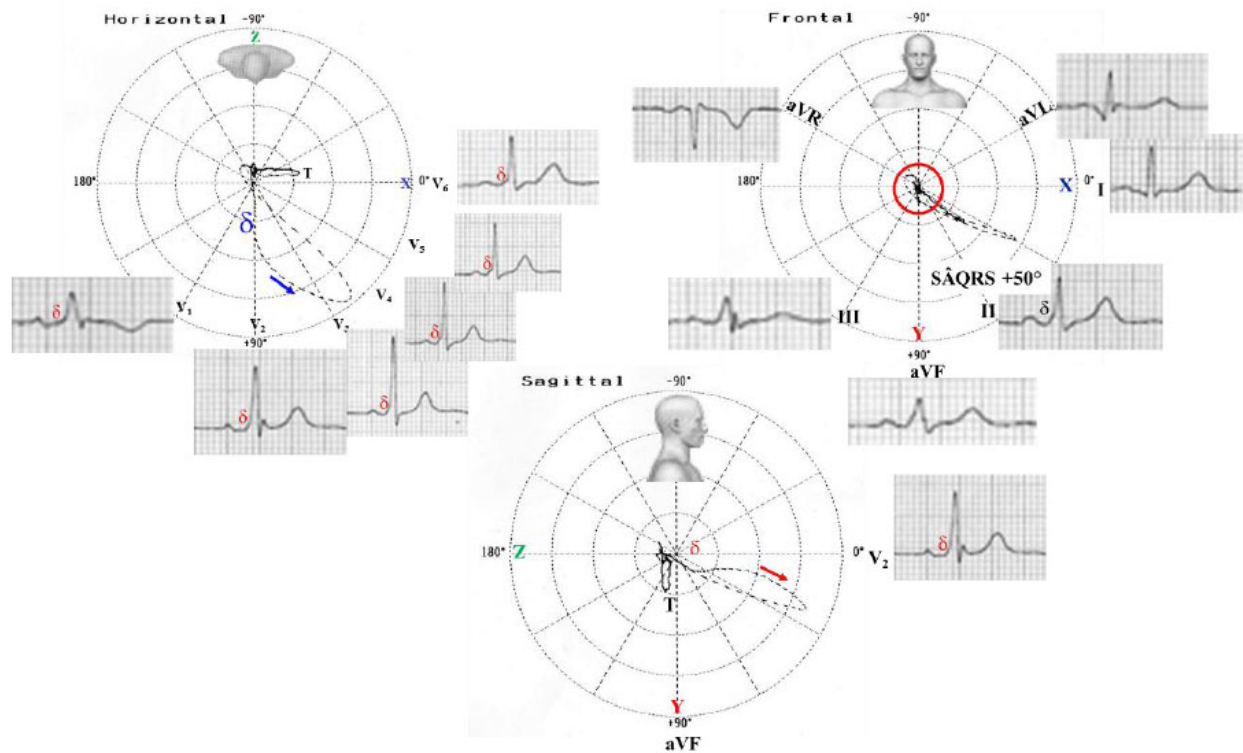


Fig. (6). Example of ventricular the pre-excitation pattern with a posterior accessory pathway. (A higher resolution / colour version of this figure is available in the electronic copy of the article).

CONCLUSION

VCG provides a three-dimensional spatial orientation of both the atrial and the ventricular activity, thereby representing a far more complete diagnostic tool than the linear ECG. Combining the two diagnostic methods (electro-vectorcardiography, ECG/VCG) enables significant gain for the differential diagnosis of several pathologies, including conduction disorders.

CONSENT FOR PUBLICATION

Not applicable.

FUNDING

None.

CONFLICT OF INTEREST

The authors have no conflicts of interest, financial or otherwise.

ACKNOWLEDGEMENTS

Declared none.

REFERENCES

- [1] Benchimol A, Desser KB, Schumacher J. Value of the vectorcardiogram for distinguishing left anterior hemiblock from inferior infarction with left axis deviation. *Chest* 1972; 61(1): 74-6. <http://dx.doi.org/10.1378/chest.61.1.74> PMID: 5049507
- [2] Lee GB, Wilson WJ, Amplatz K, Tuna N. Correlation of vectorcardiogram and electrocardiogram with coronary arteriogram. *Circulation* 1968; 38(1): 189-200. <http://dx.doi.org/10.1161/01.CIR.38.1.189> PMID: 11712288
- [3] Chou TC. When is the vectorcardiogram superior to the scalar electrocardiogram? *J Am Coll Cardiol* 1986; 8(4): 791-9. [http://dx.doi.org/10.1016/S0735-1097\(86\)80419-3](http://dx.doi.org/10.1016/S0735-1097(86)80419-3) PMID: 2944936
- [4] Hurd HP II, Starling MR, Crawford MH, Dlabal PW, O'Rourke RA. Comparative accuracy of electrocardiographic and vectorcardiographic criteria for inferior myocardial infarction. *Circulation* 1981; 63(5): 1025-9. <http://dx.doi.org/10.1161/01.CIR.63.5.1025> PMID: 7471360
- [5] de Luna AB, Massó-van Roessel A, Robledo LAE. The diagnosis and clinical implications of interatrial block. *Eur Cardiol* 2015; 10(1): 54-9. <http://dx.doi.org/10.15420/ecr.2015.10.01.54> PMID: 30310424
- [6] Escobar-Robledo LA, Bayés-de-Luna A, Lupón J, *et al.* Advanced interatrial block predicts new-onset atrial fibrillation and ischemic stroke in patients with heart failure: The "Bayes' Syndrome-HF" study. *Int J Cardiol* 2018; 271: 174-80. <http://dx.doi.org/10.1016/j.ijcard.2018.05.050> PMID: 29801761
- [7] Bayés de Luna A, Cladellas M, Oter R, *et al.* Interatrial conduction block and retrograde activation of the left atrium and paroxysmal supraventricular tachyarrhythmia. *Eur Heart J* 1988; 9(10): 1112-8. <http://dx.doi.org/10.1093/oxfordjournals.eurheartj.a062407> PMID: 3208776
- [8] Bayés de Luna A, Oter MC, Guindo J. Interatrial conduction block with retrograde activation of the left atrium and paroxysmal supraventricular tachyarrhythmias: Influence of preventive antiarrhythmic treatment. *Int J Cardiol* 1989; 22(2): 147-50. [http://dx.doi.org/10.1016/0167-5273\(89\)90061-2](http://dx.doi.org/10.1016/0167-5273(89)90061-2) PMID: 2914739
- [9] Bayes de Luna A, Fort de Ribot R, Trilla E, *et al.* Electrocardiographic and vectorcardiographic study of interatrial conduction dis-

- turbances with left atrial retrograde activation. *J Electrocardiol* 1985; 18(1): 1-13.
[http://dx.doi.org/10.1016/S0022-0736\(85\)80029-7](http://dx.doi.org/10.1016/S0022-0736(85)80029-7) PMID: 3156200
- [10] Bayés de Luna A. *The ECG for beginners*. USA: Wiley-Blackwell 2014.
- [11] Bayés de Luna A, Gusi Gené C, Soler Soler J, *et al.* *Electrocardiología clínica* (2 volúmenes). Barcelona, Spain: Cinético-Médica 1977.
- [12] Bayés de Luna A, Platonov P, Cosio FG, *et al.* Interatrial blocks. A separate entity from left atrial enlargement: A consensus report. *J Electrocardiol* 2012; 45(5): 445-51.
<http://dx.doi.org/10.1016/j.jelectrocard.2012.06.029> PMID: 22920783
- [13] Baranchuk A, Bayes-Genis A. Bayés' syndrome. *Rev Esp Cardiol (Engl Ed)* 2016; 69(4): 439.
<http://dx.doi.org/10.1016/j.rec.2015.12.013> PMID: 26948392
- [14] Ariyaratnam V, Spodick DH. Advanced interatrial block: A classic electrocardiogram. *Cardiology* 2005; 104(1): 33-4.
<http://dx.doi.org/10.1159/000086052> PMID: 15942182
- [15] Waldo AL, Vitikainen KJ, Hoffman BF. The sequence of retrograde atrial activation in the canine heart. Correlation with positive and negative retrograde P waves. *Circ Res* 1975; 37(2): 156-63.
<http://dx.doi.org/10.1161/01.RES.37.2.156> PMID: 1149190
- [16] Spodick DH, Ariyaratnam V, Apiyasawat S. Higher prevalence of cardiovascular events among patients with abnormal atrial depolarization and coronary artery disease at 18 months' post-exercise tolerance testing. *Am Heart Hosp J* 2007; 5(4): 236-40.
<http://dx.doi.org/10.1111/j.1541-9215.2007.07361.x> PMID: 17982305
- [17] Miquel C, Sodi-Pallares D, Cisneros F, Pileggi F, Medrano GA, Bisteni A. Right bundle branch block and right ventricular hypertrophy; electrocardiographic and vectorcardiographic diagnosis. *Am J Cardiol* 1958; 1(1): 57-67.
[http://dx.doi.org/10.1016/0002-9149\(58\)90076-6](http://dx.doi.org/10.1016/0002-9149(58)90076-6) PMID: 13497956
- [18] Bussink BE, Holst AG, Jespersen L, Deckers JW, Jensen GB, Prescott E. Right bundle branch block: prevalence, risk factors, and outcome in the general population: Results from the Copenhagen City Heart Study. *Eur Heart J* 2013; 34(2): 138-46.
<http://dx.doi.org/10.1093/eurheartj/ehs291> PMID: 22947613
- [19] de Micheli A, Medrano GA, Martínez Rios MA. Right blocks in interauricular communication. *Arch Inst Cardiol Mex* 1978; 48(6): 1091-113.
 PMID: 727842
- [20] Tabatabaei N, Katanyuwong P, Breen JF, *et al.* Images in cardiovascular medicine. Uncommon variant of Ebstein anomaly with tricuspid stenosis. *Circulation* 2009; 120(1): e1-2.
<http://dx.doi.org/10.1161/CIRCULATIONAHA.108.835652> PMID: 19581515
- [21] Hébert JL, Duthoit G, Hidden-Lucet F, *et al.* Images in cardiovascular medicine. Fortuitous discovery of partial Uhl anomaly in a male adult. *Circulation* 2010; 121(22): e426-9.
<http://dx.doi.org/10.1161/CIRCULATIONAHA.110.960773> PMID: 20530016
- [22] Gelband H, Waldo AL, Kaiser GA, Bowman FO Jr, Malm JR, Hoffman BF. Etiology of right bundle-branch block in patients undergoing total correction of tetralogy of Fallot. *Circulation* 1971; 44(6): 1022-33.
<http://dx.doi.org/10.1161/01.CIR.44.6.1022> PMID: 5127831
- [23] Krongrad E, Hefler SE, Bowman FO Jr, Malm JR, Hoffman BF. Further observations on the etiology of the right bundle branch block pattern following right ventriculotomy. *Circulation* 1974; 50(6): 1105-13.
<http://dx.doi.org/10.1161/01.CIR.50.6.1105> PMID: 4430109
- [24] Riera AR, de Cano SJ, Cano MN, Gimenez VM, de Padua Fleury Neto LA, Sousa JE. Vector electrocardiographic alterations after percutaneous septal ablation in obstructive hypertrophic cardiomyopathy. Possible anatomic causes. *Arq Bras Cardiol* 2002; 79(5): 466-75.
<http://dx.doi.org/10.1590/s0066-782x2002001400004> PMID: 12447497
- [25] Tomita M, Kitazawa H, Sato M, Okabe M, Antzelevitch C, Aizawa Y. A complete right bundle-branch block masking Brugada syndrome. *J Electrocardiol* 2012; 45(6): 780-2.
<http://dx.doi.org/10.1016/j.jelectrocard.2012.06.019> PMID: 22832153
- [26] Zamfirescu NR, Ciplea A, Filcescu V, *et al.* Right branch block associated with anterior left hemiblock; electrocardiographic and vectorcardiographic aspects. *Physiology* 1978; 15(4): 269-78.
 PMID: 106412
- [27] Retamal E, Illanes A, Moreno J. Vectorcardiographic study of 15 patients with anterior left hemiblock and right branch block. *Rev Med Chil* 1972; 100(9): 1077-81.
 PMID: 4644071
- [28] Medrano GA, Brenes C, De Micheli A, Sodi-Pallares D. Block of the anterior subdivision of the left bundle-branch, isolated or combined with right bundle-branch block. Clinical, electro and vectorcardiography studies. *Arch Inst Cardiol Mex* 1969; 39(5): 672-87.
 PMID: 5374309
- [29] Cergueira-Gomes M, Correia-dos-Santos J, Paula-Pinto R, Abreu-Lima C, Ramalhão C, Rocha-Gonçalves F. Right bundle branch block combined with left axis deviation: A vectorcardiographic study of 48 cases. *J Electrocardiol* 1972; 5(2): 127-34.
[http://dx.doi.org/10.1016/S0022-0736\(72\)80028-1](http://dx.doi.org/10.1016/S0022-0736(72)80028-1) PMID: 4260729
- [30] Lichstein E, Chadda KD, Gupta PK. Complete right bundle branch block with left axis deviations: Significance of vectorcardiographic morphology. *Am Heart J* 1973; 86(1): 13-22.
[http://dx.doi.org/10.1016/0002-8703\(73\)90004-5](http://dx.doi.org/10.1016/0002-8703(73)90004-5) PMID: 4268305
- [31] Dubner S, Schapachnik E, Riera AR, Valero E. Chagas disease: State-of-the-art of diagnosis and management. *Cardiol J* 2008; 15(6): 493-504.
 PMID: 19039752
- [32] Ribeiro AL, Marcolino MS, Prineas RJ, Lima-Costa MF. Electrocardiographic abnormalities in elderly Chagas disease patients: 10-year follow-up of the Bambuí Cohort Study of Aging. *J Am Heart Assoc* 2014; 3(1)e000632
<http://dx.doi.org/10.1161/JAHA.113.000632> PMID: 24510116
- [33] Villongco CT, Krummen DE, Stark P, Omens JH, McCulloch AD. Patient-specific modeling of ventricular activation pattern using surface ECG-derived vectorcardiogram in bundle branch block. *Prog Biophys Mol Biol* 2014; 115(2-3): 305-13.
<http://dx.doi.org/10.1016/j.pbiomolbio.2014.06.011> PMID: 25110279
- [34] Rodríguez-Padial L, Rodríguez-Picón B, Jerez-Valero M, *et al.* Diagnostic accuracy of computer-assisted electrocardiography in the diagnosis of left ventricular hypertrophy in left bundle branch block. *Rev Esp Cardiol (Engl Ed)* 2012; 65(1): 38-46.
<http://dx.doi.org/10.1016/j.rec.2011.07.017> PMID: 22100804
- [35] Liakopoulos V, Kellerth T, Christensen K. Left bundle branch block and suspected myocardial infarction: Does chronicity of the branch block matter? *Eur Heart J Acute Cardiovasc Care* 2013; 2(2): 182-9.
<http://dx.doi.org/10.1177/2048872613483589> PMID: 24222829
- [36] Brembilla-Perrot B, Alla F, Suty-Selton C, *et al.* Nonischemic dilated cardiomyopathy: Results of noninvasive and invasive evaluation in 310 patients and clinical significance of bundle branch block. *Pacing Clin Electrophysiol* 2008; 31(11): 1383-90.
<http://dx.doi.org/10.1111/j.1540-8159.2008.01199.x> PMID: 18950294
- [37] Chan DD, Wu KC, Loring Z, *et al.* Comparison of the relation between left ventricular anatomy and QRS duration in patients with cardiomyopathy with *versus* without left bundle branch block. *Am J Cardiol* 2014; 113(10): 1717-22.
<http://dx.doi.org/10.1016/j.amjcard.2014.02.026> PMID: 24698465
- [38] Poels TT, Houthuizen P, Van Garsse LA, Maessen JG, de Jaegere P, Prinzen FW. Transcatheter aortic valve implantation-induced left bundle branch block: Causes and consequences. *J Cardiovasc Transl Res* 2014; 7(4): 395-405.
<http://dx.doi.org/10.1007/s12265-014-9560-x> PMID: 24800873
- [39] Silva JA, Khuri B, Barbee W, Fontenot D, Cheirif J. Systolic excursion of the mitral annulus to assess septal function in paradoxical septal motion. *Am Heart J* 1996; 131(1): 138-45.
[http://dx.doi.org/10.1016/S0002-8703\(96\)90062-9](http://dx.doi.org/10.1016/S0002-8703(96)90062-9) PMID:

- 8554000
- [40] Bharati S, Lev M, Dhingra RC, Chuquimia R, Towne WD, Rosen KM. Electrophysiologic and pathologic correlations in two cases of chronic second degree atrioventricular block with left bundle branch block. *Circulation* 1975; 52(2): 221-9. <http://dx.doi.org/10.1161/01.CIR.52.2.221> PMID: 125157
- [41] Kyndt F, Probst V, Potet F, *et al.* Novel SCN5A mutation leading either to isolated cardiac conduction defect or Brugada syndrome in a large French family. *Circulation* 2001; 104(25): 3081-6. <http://dx.doi.org/10.1161/hc5001.100834> PMID: 11748104
- [42] Asatryan B, Medeiros-Domingo A. Molecular and genetic insights into progressive cardiac conduction disease. *Europace* 2019; 21(8): 1145-58. <http://dx.doi.org/10.1093/europace/euz109> PMID: 31087102
- [43] Mavrogeni S, Karabela G, Stavropoulos E, *et al.* Heart failure imaging patterns in systemic lupus erythematosus. Evaluation using cardiovascular magnetic resonance. *Int J Cardiol* 2014; 176(2): 559-61. <http://dx.doi.org/10.1016/j.ijcard.2014.07.016> PMID: 25049017
- [44] Rowinsky EK, McGuire WP, Guarnieri T, Fisherman JS, Christian MC, Donehower RC. Cardiac disturbances during the administration of taxol. *J Clin Oncol* 1991; 9(9): 1704-12. <http://dx.doi.org/10.1200/JCO.1991.9.9.1704> PMID: 1678781
- [45] Bellavia D, Pellikka PA, Abraham TP, *et al.* 'Hypersynchronisation' by tissue velocity imaging in patients with cardiac amyloidosis. *Heart* 2009; 95(3): 234-40. <http://dx.doi.org/10.1136/hrt.2007.140343> PMID: 18474536
- [46] Strauss DG, Selvester RH, Wagner GS. Defining left bundle branch block in the era of cardiac resynchronization therapy. *Am J Cardiol* 2011; 107(6): 927-34. <http://dx.doi.org/10.1016/j.amjcard.2010.11.010> PMID: 21376930
- [47] Manohar N, Young ML. Rate dependent bundle branch block induced by hyperkalemia. *Pacing Clin Electrophysiol* 2003; 26(9): 1909-10. <http://dx.doi.org/10.1046/j.1460-9592.2003.00291.x> PMID: 12930511
- [48] Al-Hadi H, Sallam M. Symptomatic permanent left bundle branch block (LBBB) complicating diagnostic left heart catheterization. *Sultan Qaboos Univ Med J* 2010; 10: 114-9.
- [49] Castellanos A Jr, Chapunoff E, Castillo CA, Arcebal AG, Lemberg L. The vectorcardiogram in left posterior hemiblock associated with inferior wall myocardial infarction. *Chest* 1972; 61(3): 221-7. <http://dx.doi.org/10.1378/chest.61.3.221> PMID: 5021166
- [50] Pérez-Riera AR, Barbosa-Barros R, Daminello-Raimundo R, de Abreu LC, Nikus K. The tetrafascicular nature of the intraventricular conduction system. *Clin Cardiol* 2019; 42(1): 169-74. <http://dx.doi.org/10.1002/clc.23093> PMID: 30294894
- [51] Damjanović MR, Dordević-Radojković D, Perišić Z, *et al.* Ebstein's anomaly as a cause of paroxysmal atrial fibrillation. *Vojnosanit Pregl* 2008; 65(11): 847-50. <http://dx.doi.org/10.2298/VSP0811847D> PMID: 19069718